Fast Rigorous Analysis of Shielded Planar Filters

C. J. Railton, *Member, IEEE,* and S. A. Meade

Abstract—**Much interest has been shown by industry and in the literature regarding the analysis of complex planar components such as are found in modern (M)MIC's. Many of the published results have, however, required the use of a large computer. In this contribution a technique is described whereby rigorous analyses of moderately complex planar circuits may be obtained on a relatively small desktop computer. Results obtained using a personal computer are presented for several planar filter geometries. These are in good agreement with published results which use more computationally expensive techniques.**

Introduction

THE REQUIREMENT to predict the behavior of planar microwave components and circuits has existed for many years. Recently, however, as the complexity, component density and operating frequencies of these circuits has increased dramatically, the problems posed to the designers of CAD tools have become much more difficult. No longer is it adequate to treat a circuit as a set of isolated components or to use models based on quasi-static formulations. The interactions between different parts of a circuit make it necessary to perform a rigorous full wave analysis which takes into account all the couplings which exist. A number of techniques are available which are capable, in principle, of providing such a rigorous solution to almost any electromagnetic problem, including the analysis of microstrip circuits. These include the Spectral Domain Method [1], [2], [8], [10], Finite Difference Time Domain [3], [9], [12], Transmission Line Matrix [4], Bergeron's Method [5], [11], and Space Domain Methods [6]. They are, however, all limited by the requirement for a large amount of computer resources. Notwithstanding the rapid increase in the availability of computer power, work is still necessary to increase the efficiency of the algorithms used. In this contribution, a technique is described which is capable of characterizing microwave circuits, such as filters, using only a small desk-top computer. The technique which is based on the Spectral Domain Method (SDM), exploits the asymptotic behavior both of the Green's function for the shielded slab-loaded waveguide and of the current distribution in the vicinity of electrically small geometrical features, such as edges and corners, in order to speed up the computation and to reduce the number of unknowns required.

Manuscript received August 2, 1991; revised November 15, 1991.

The authors are with the Center for Communications Research, Faculty of Engineering, University of Bristol, Bristol, BS8 1TR, United Kingdom.

IEEE Log Number 9106766.

The Spectral Domain Method

Analyses of complex planar circuits using various implementations of the SDM are well described in the literature e.g. [1], [2], [7]. In many of these treatments, the unknown currents on the metal parts of the circuit are expressed as a linear combination of a set of basis functions, often rooftop functions. Making use of the slab-loaded waveguide Green's function, the unknown current coefficients can be found using the Method of Moments. This may be done either in the spectral domain or the space domain [6]. Either approach requires the calculation of the elements of a large impedance matrix followed by the solution of the resulting set of simultaneous equations. Unfortunately, the amount of computer time and memory required by this process increases very rapidly with the complexity of the geometry being analysed. This means that a level of complexity is reached at which it rapidly becomes impractical to use the SDM in its basic form. Once this point is reached, means of enhancing the basic method are essential. This is particularly important in modern densely packed microwave integrated circuits where interactions between components cannot satisfactorily be ignored. One such enhancement which has already been described in connection with open structures [1], [7], is the exploitation of the redundancy inherent in the impedance matrix in order to reduce the number of calculations which need to be performed. Recently, the use of the Fast Fourier Transform (FFT) has been reported [2] to speed up the calculation of the impedance matrix elements. In this contribution, the basic method will be further enhanced in two ways: Firstly the calculation of the impedance matrix elements is greatly sped up by using asymptotic forms of both the Green's functions and the rooftop basis functions, in conjunction with the FFT. Using this technique, it is necessary to calculate only five 2-D fast fourier transforms, and this only once for each geometry. In contrast to this, in [2], twelve 2-D FFT's must be calculated for each frequency point. Secondly, a means will be described for reducing the number of unknowns in the formulation by using basis functions which incorporate *a priori* knowledge of the current distribution.

Fast Calculation of the Impedance Matrix

The Method of Moments formulated in the spectral domain and applied to a planar structure leads to a set of equations of the following form:

$$\sum_s a_s Z_{st} = V_t \quad \text{for all } t \tag{1}$$

where the elements of the impedance matrix are

$$\boldsymbol{Z}_{st} = \sum_{n,m} \tilde{\boldsymbol{w}}_t(n, m)\, \tilde{\boldsymbol{G}}(n, m, \omega)\, \tilde{\boldsymbol{J}}_s(n, m) \tag{2}$$

and the excitation vector is given by

$$\boldsymbol{V}_t = \sum_{n,m} \tilde{\boldsymbol{w}}_t(n, m)\, \tilde{\boldsymbol{E}}_i(n, m). \tag{3}$$

$\boldsymbol{E}_i$ is the incident electric field.
$\{\boldsymbol{J}_s(x, y)\}$ is the set of current basis functions
$\{\boldsymbol{w}_t(x, y)\}$ is the set of weighting functions
$\underset{\sim}{\boldsymbol{G}}(\omega)$ is the dyadic Green's function
indicates the Fourier transform and the total current is given by $\boldsymbol{J}(x, y) = \Sigma\, a_s \boldsymbol{J}_s(x, y)$.

This set of equations may be solved for the unknown current in the structure, hence the unknown fields around the structure may also be found.

Since each element of the Z matrix requires the evaluation of a doubly infinite summation and a typical problem may involve several hundred unknowns, a means is required to perform this calculation efficiently. We may rearrange the characteristic equation by making use of the asymptotic properties of the Green's function, described in [10] for the case of a two layer structure and in [8] for the case of a three layer structure containing a thin passivation layer:

$$\boldsymbol{Z}_{st} = \sum_{n}^{N_1} \sum_{m}^{M_1} \tilde{\boldsymbol{w}}_t(n, m)(\tilde{\boldsymbol{G}}(n, m, \omega) - \tilde{\boldsymbol{G}}^{\infty}(n, m))\, \tilde{\boldsymbol{J}}_s(n, m) + \tilde{\boldsymbol{G}}_1^{\infty}\tilde{\boldsymbol{Z}}_{st}^{\infty} \tag{4}$$

where

$$\boldsymbol{Z}_{st}^{\infty} = \sum_{n}^{N_2} \sum_{m}^{M_2} \tilde{\boldsymbol{w}}_t(n, m)\, \tilde{\boldsymbol{G}}_2^{\infty}(n, m)\, \tilde{\boldsymbol{J}}_s(n, m)$$

$\tilde{\boldsymbol{G}}^{\infty}(n, m) = \boldsymbol{G}_1^{\infty}\tilde{\boldsymbol{G}}_2^{\infty}$ is the asymptotic form of the Green's function for large n and m and is independent of ω, $\boldsymbol{G}_1^{\infty}$ is a function of the geometry and $\tilde{\boldsymbol{G}}_2^{\infty}(n, m)$ is independent both of geometry and frequency.

The first summation of (4) converges rapidly and, therefore, few terms of the series need be evaluated. The summation for $\boldsymbol{Z}^{\infty}$ is independent of frequency and need be evaluated only once for each geometry. In spite of this, since N_2 and M_2 must be of the order of 1000 for good convergence, the calculation of the second summation can take a prohibitive amount of time and a more efficient means of evaluation must be found.

For a class of sub-domain basis functions and weighting functions, including the rooftop functions used in [1], [2], [6], [7], it is possible to express the second summation in the following form:

$$\boldsymbol{Z}_{st}^{\infty} = \sum_{n,m} \tilde{\boldsymbol{F}}(n, m)\, T\left(\frac{n\pi x_s}{a}\right) T\left(\frac{n\pi y_s}{b}\right) \cdot T\left(\frac{n\pi x_t}{a}\right) T\left(\frac{n\pi y_t}{b}\right) \tag{5}$$

where $\tilde{\boldsymbol{F}}(n, m)$ is a known function of n and m but not of s and t, provided that all the basis functions are the same apart from a spatial translation. The functions T can be either $\pm$Sin or Cos and a and b are the dimensions of the box (see Fig. 1(a)). The derivation of this equation for the case of rooftop basis functions is given in the appendix.

Equivalently we may say:

$$\boldsymbol{Z}_{st}^{\infty} = \sum_{n,m} \frac{\tilde{\boldsymbol{F}}(n, m)}{4} \left\{ T\left(\frac{n\pi(x_s - x_t)}{a}\right) + T\left(\frac{n\pi(x_s + x_t)}{a}\right)\right\}\left\{ T\left(\frac{n\pi(y_s - y_t)}{b}\right) + T\left(\frac{n\pi(y_s + y_t)}{b}\right)\right\} \tag{6}$$

Thus the problem is reduced to the calculation of summations of the form:

$$\sum_{n,m} \tilde{\boldsymbol{F}}(n, m)\, T\left(\frac{n\pi(x_s \pm x_t)}{a}\right) T\left(\frac{m\pi(y_s \pm y_t)}{b}\right) \tag{7}$$

for all values of the sums and differences of the positions of the rooftop functions.

Comparing this expression with the two dimensional DFT we see that *all* elements in the matrix $\boldsymbol{Z}^{\infty}$ may be efficiently calculated using the FFT algorithm provided we restrict the geometry such that:

$$\frac{x_s \pm x_t}{a}(N + 1) \quad \text{and} \quad \frac{y_s \pm y_t}{b}(N + 1)$$

are integers for all s and t, where N is the number of points in the FFT.

In practice, once one has accepted the restriction of keeping the finite element sizes the same, this extra restriction is not severe.

In order to avoid recalculation of the summations given by (7) each time the metallization pattern is changed, one may set up a data file containing the calculated sums for all possible values of $(x_s \pm x_t, y_s \pm y_t)$ for a specified box size and finite element size. For each metallization under analysis, the required values can be read from the data file and $\boldsymbol{Z}^{\infty}$ quickly calculated. We consider it better to store these values rather than the corresponding values for $\boldsymbol{Z}$ as described in [7] for the reason that $\boldsymbol{Z}^{\infty}$ is independent of frequency, dielectric constant and thickness and the number of dielectric layers. Moreover the storage requirement for multilayered structures is no greater than for a single dielectric if $\boldsymbol{Z}^{\infty}$ is stored. This is not the case if $\boldsymbol{Z}$ is stored. The penalty in having to recalculate the first summation in (2) is not great since N_1 and M_1 may be as low as 20.

We are now in a position to calculate the elements of $\boldsymbol{Z}^{\infty}$. First the two dimensional DFT's of the functions $\tilde{\boldsymbol{F}}(n, m)$ are calculated using the FFT algorithm, secondly the elements of $\boldsymbol{Z}^{\infty}$ are evaluated using (8):

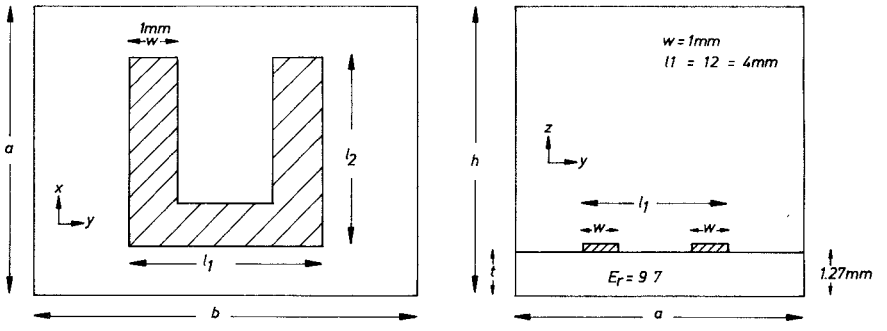

(a) (b)

Fig. 1. (a) Plan of a boxed hairpin resonator. (b) Elevation of a boxed hairpin resonator.

$$Z_{st}^{\infty} = \pm 0.25F\left(\frac{x_s - x_t}{a}, \frac{y_s - y_t}{b}\right) \pm 0.25F\left(\frac{x_s + x_t}{a}, \frac{y_s - y_t}{b}\right) \pm 0.25F\left(\frac{x_s - x_t}{a}, \frac{y_s + y_t}{b}\right) \pm 0.25F\left(\frac{x_s + x_t}{a}, \frac{y_s + y_t}{b}\right) \quad (8)$$

Analysis of a Hairpin Resonator

In order to demonstrate the efficiency obtainable by using this method of calculating the Z matrix, the hairpin resonator geometry shown in Fig. 1 was investigated. This type of resonator is well suited for the construction of miniature band-pass filters at X band and below. Because of the strong interaction between the different parts of the structure, however, the results obtainable from the widely used microwave CAD tools are likely to be unreliable. The dimensions used were as follows: $l_1 = l_2 = 4$ mm, $w = 1$ mm, $t = 1.27$ mm, $h = 12.7$ mm. The effect on the resonant frequency of the hairpin resulting from varying the dimensions a and b of the enclosing box was investigated. This is of interest since it shows how small an enclosure may be used without significantly altering the behavior of the resonator. In addition the convergence of the result as the number of finite elements was increased was investigated.

Fig. 2 shows the calculated resonant frequency of a hairpin resonator having the geometry of Fig. 1 for various sizes of the enclosing box and for various numbers of finite elements. For comparison, the same structures were analysed using the Finite Difference Time Domain (FDTD) method [9] which has been shown to be a reliable and accurate full-wave technique for the analysis of planar components. It can be seen that there is very good agreement between the methods. The results for this structure were also obtained using a widely available commercial microwave CAD tool and were found to be approximately 10% in error. This is almost certainly due to the effect of the coupling between the two right angle corners which is

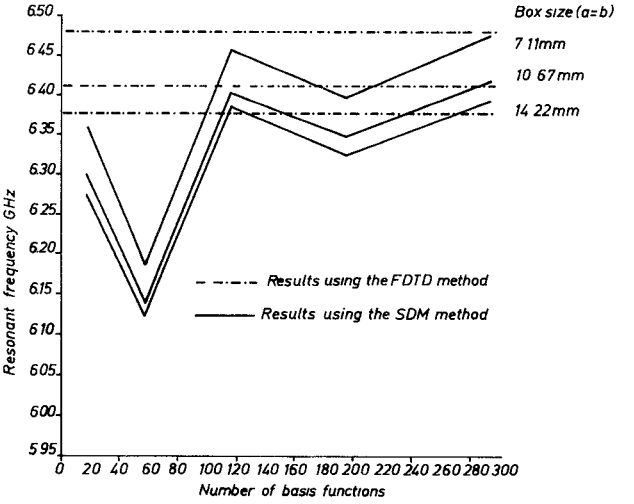

Fig. 2. Convergence of the SDM for various box sizes.

ignored in the CAD tool but included automatically in the SDM and the FDTD methods. This emphasizes the importance of using a rigorous analysis even for components as comparatively simple as the hairpin resonator at 6.5 GHz. Although the computer time to analyse this structure is still significant, it nonetheless represents an improvement over the basic method of at least an order of magnitude for a given accuracy.

It is noted that the convergence pattern for the SDM is oscillatory. This is due to the fact that the nature of the approximation is different depending on whether an even or an odd number of rooftop functions are used to describe the transverse variation of current.

We can see that, for this structure, a very large number of finite elements is required for convergence. It is noted that the convergence curves are oscillatory. This is because the situation where there is an even number of elements across the track is different from that where there is an odd number. We can also see that, the convergence curves are very nearly parallel, hence the error due to finite element size is almost independent of the size of the box. Similar effects have been previously observed [9], and can be explained physically by the fact that the current distribution on the metal does not depend greatly on the surrounding geometry unless strong coupling exists.

This fact may be exploited in a number of ways to further increase efficiency and allow the analysis of more complex structures such as multi-element filters.

Use of Pre-Computed Basis Functions

A plot of the calculated current distribution for the first resonant mode of the hairpin is shown in Fig. 3. No smoothing has been applied, hence the apparent discontinuities of current density in the transverse directions. It can be seen that the current distribution is dominated by the effects of the edges and the corners. These effects are insensitive to the environment. We can make use of the relative invariance of the current distribution in order to greatly speed up the calculations described in the previous section as well as allowing the solution of much more complicated problems. Although this phenomenon has been widely exploited for two dimensional analyses, e.g., [10], where analytical expressions for the distributions are available, it has rarely been used in conjunction with a three dimensional analysis and, to the authors' knowledge, never with the generality of the present approach. For a structure such as the hairpin, we can expand the unknown current as a linear combination of its resonant modes:

$$\boldsymbol{J}(\boldsymbol{r}) = \sum_{p=1}^{P} b_p \psi_p(\boldsymbol{r}) \tag{9}$$

where $\psi_p(\boldsymbol{r})$ is the current distribution associated with the pth resonant mode. For most cases of practical interest the summation can be truncated after only a few terms, in some cases only one term is required. From the finite element method we can find these distributions as a linear combination of the original rooftop basis functions:

$$\psi_p(\boldsymbol{r}) = \sum_{q=1}^{Q} a_{pq} \boldsymbol{R}_q(\boldsymbol{r}) \tag{10}$$

where $\boldsymbol{R}_q(\boldsymbol{r})$ is the qth rooftop function as defined in the appendix. Q is the total number of finite elements in the basic analysis and can be of the order of hundreds. Alternatively, for some structures, ψ_p may be known analytically. In these cases the set $\{a_p\}$ can be calculated using a least squares approximation.

The total current is therefore given by

$$\boldsymbol{J}(\boldsymbol{r}) = \sum_{p}^{P} \sum_{q}^{Q} b_p a_{pq} \boldsymbol{R}_q(\boldsymbol{r}). \tag{11}$$

The coefficients, a_{pq}, are calculated once for each hairpin geometry, thereafter we need only calculate the much smaller number of b's. The size of the impedance matrix for these subsequent cases is only $2S \times 2S$ and the matrix may therefore be solved with great rapidity. Because we have expressed $\{\psi_p\}$ as a linear combination of rooftop functions, the elements of the asymptotic Z matrix can be expressed as follows:

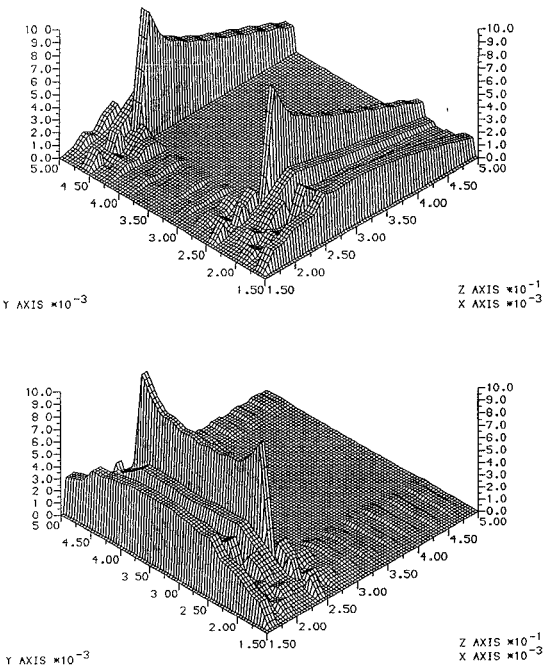

Fig. 3. Current distribution of the first resonant mode of a hairpin resonator.

$$Z_{st}^{\infty} = \sum_{p} \sum_{q} a_{pq} \sum_{n,m} \frac{\tilde{F}(n, m)}{4} \cdot \left\{ \left\{ T\left(\frac{n\pi(x_p - x_q)}{a}\right) + T\left(\frac{n\pi(x_p + x_q)}{a}\right) \right\} \cdot \left\{ T\left(\frac{n\pi(y_p - y_q)}{b}\right) + T\left(\frac{n\pi(y_p + y_q)}{b}\right) \right\} \right\} \tag{12}$$

which, as before, can be expressed as a summation of terms of the form of (7). Thus full advantage can be taken of the method described in the appendix to efficiently calculate the Z matrix.

Consider the structure shown in Fig. 4. This is a pair of hairpin resonators such as may form part of a miniature bandpass filter.

In this case we use basis functions as follows:

$$\boldsymbol{J}(\boldsymbol{r}) = \sum_{p} b_{p1} \psi_p(\boldsymbol{r} + \boldsymbol{r}_1) + \sum_{p} b_{p2} \psi_p(\boldsymbol{r} + \boldsymbol{r}_2) \tag{13}$$

where $\boldsymbol{r}_1$ and $\boldsymbol{r}_2$ are the positions of hairpins one and two relative to the position of the hairpin used to calculate $\{\psi_p\}$. The size of the impedance matrix for the complete circuit is still only $4S \times 4S$.

For filter design, we need to know both the resonant frequency of the individual elements and also the coupling coefficient as a function of the separation, s. The latter may be calculated from a knowledge of the resonant frequencies of the even and odd modes of the coupled resonators. Since we are only considering the response of the circuit close to the fundamental resonances, we need only take a single term in the sums of (13). Fig. 5 shows the results using the pre-calculated basis functions com-

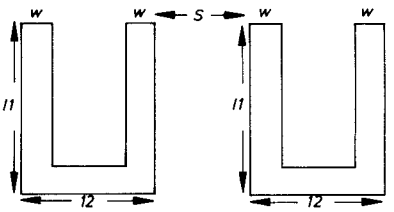

Fig. 4. Coupled hairpin resonators.

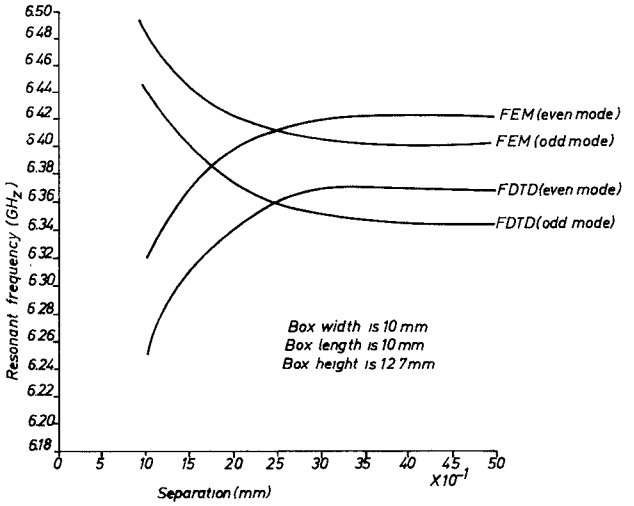

Fig. 5. Resonant frequencies of two coupled hairpin resonators as a function of separation.

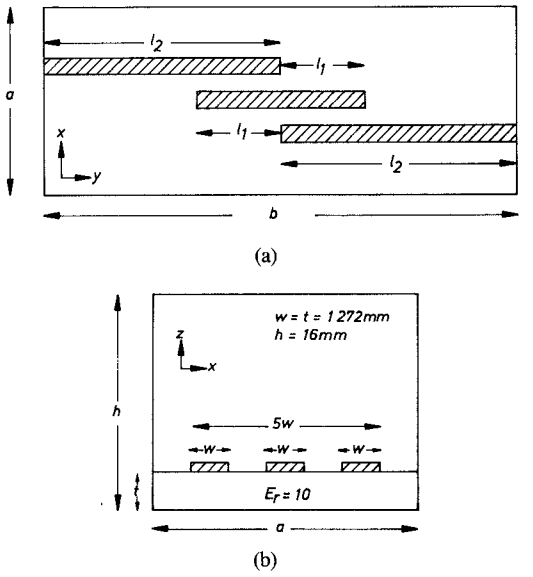

Fig. 6. (a) Plan of boxed edge-coupled bandpass filter. (b) Elevation of boxed filter. $l_1 = 6.36$ mm, $l_2 = (b/2) = 8.48$ mm, $a = 11.62$ mm.

pared with similar results calculated using the basic SDM using 234 elements and results obtained using the FDTD technique [12]. It can again be seen that there is good agreement between the methods of better than 1% in the absolute resonant frequency and excellent agreement in the coupling coefficient. It is noted that, due to the small size of the enclosure, there is interaction between the resonators and the box which results in the plots of the resonant frequencies of the even and odd modes crossing when the resonators are widely separated.

The Analysis of an Edge Coupled Band Pass Filter

Consider the filter shown in Fig. 6. In the literature results for this filter are available from measurements performed by Shibata *et al.* [11], from a quasi-static analysis and from a rigorous analysis based on Bergeron's method [11]. In addition results are available from a rigorous analysis based on the FDTD method [12]. This structure has been analyzed using the present method in order to assess the efficiency and accuracy obtainable.

The analysis is approached in three stages.

i) The transverse current distribution on the three microstrip lines is pre-calculated. This is carried out using a 2-D version of the technique. From this we get the transverse current distribution in the form shown in (10).

ii) We now consider the microstrip resonator in isolation and we use the technique to calculate the longitudinal current distributions corresponding to the first few resonant modes. In this calculation we use the transverse current distribution derived in step 1. The resulting current distributions are shown in Fig. 7. These form the basis functions, $\psi_p(r)$ in (10), used to describe the microstrip resonator in the next stage.

iii) Now the complete structure is analyzed. The transverse current distribution on the feed lines is assumed to be the same as that obtained in stage 1 and the current distribution on the resonator is expanded as a linear combination of the functions obtained in stage 2. Note that only 3 basis functions ($Q = 3$ in (10)) are required to fully describe the strip resonator over the frequency range of interest. Moreover, if we wished to consider an n element filter we would require only $3n$ basis functions. Moreover stages one and two need be carried out only once per resonant structure.

In total, 67 basis functions ($P = 67$ in (9)) are required for the structure shown in Fig. 6. In contrast to this, 333 rooftop functions would be required in the basic method for equivalent accuracy. This allows a large saving in computation time per frequency. The run time on a Gould NP1, using non-optimized code, of approximately 15 min to calculate Z^{∞}, (8), and a further 80 s to calculate S-parameters at each spot frequency was measured. These computer times indicate that it is entirely practicable to carry out optimization on a multi-stage filter.

Fig. 8 shows the results, which we have obtained, for mag [$S21$] plotted against frequency. For comparison the measured results of Shibata *et al.* [loc cit] for the corresponding open structure are also plotted. A frequency shift, from the measured reference, of approximately 0.1 GHz is evident and also a higher predicted rejection below 4 GHz. The offset in the resonant frequencies is due to the fact that the shielding enclosure is not taken into account in reference [11]. To show that these discrepancies are indeed due to the shield walls we calculated the

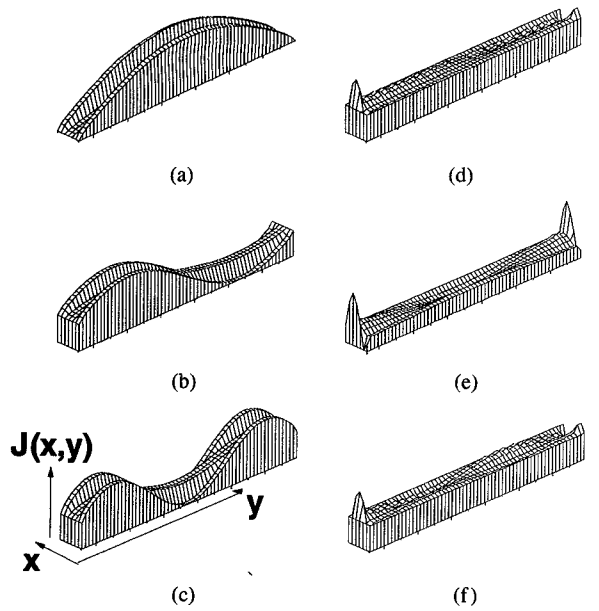

Fig. 7. Current distributions for the first three resonant modes of a strip resonator. (a)–(c): y-directed current. (d)–(f): corresponding x-directed.

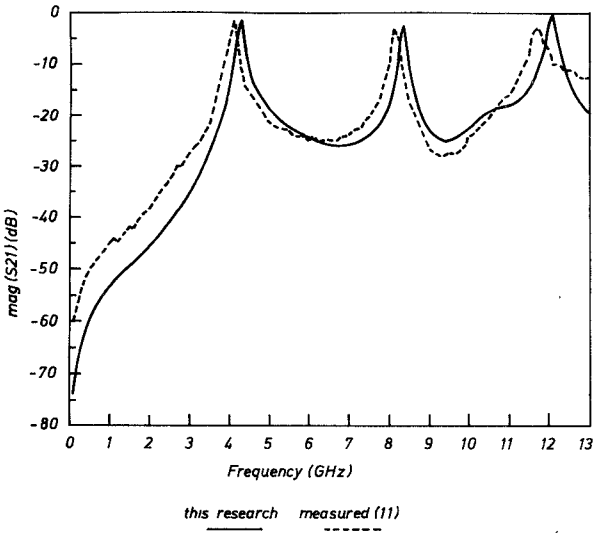

Fig. 8. S-parameter $|S21|$ for edge coupled filter.

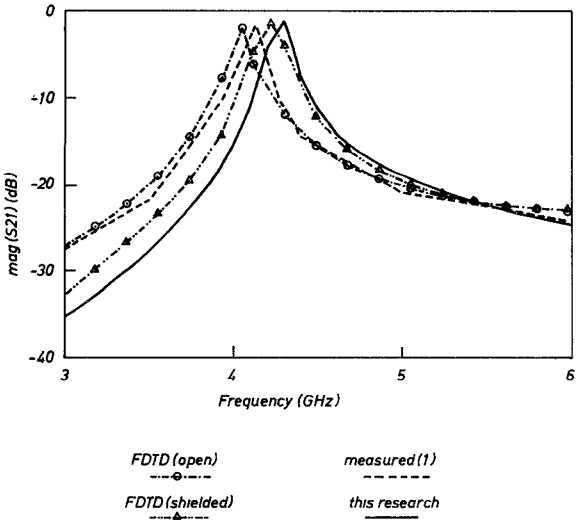

Fig. 9. S-parameter $|S21|$ for edge coupled filter—comparison with FDTD.

S-parameters for both open and partially shielded (cover and side walls only) structures using the FDTD method [12]. Fig. 9 shows a plot of mag [$S21$] over the frequency range 3 GHz to 6 GHz, which includes the first resonant peak. The results predicted by the FDTD for the open structure is close to the measured [11] whereas the corresponding results for the shielded structure agrees more closely with the predictions of this research. Any further discrepancies could be explained by the proximity of the end walls which are not included in the FDTD model or the measurements, and by the limited frequency resolution available from the FDTD model.

Conclusion

We have shown that realistically complex microstrip circuits can be rigorously analysed on a small computer by means of the spectral domain technique in combination with pre-computed basis functions and the use of the asymptotic forms of the Green's function and the FFT algorithm. The results compare well with published measurements and with calculations using the FDTD method.

Appendix
Calculation of the Asymptotic Z Matrix

The rooftop basis functions can be expressed as follows:

$$J_{xn}(x, y) = 1 - |x - x_n|/l_x \qquad x_n - l_x < x < x_n + l_x,\quad y_n - l_y < y < y_n + l_y$$
$$= 0 \qquad \text{otherwise}$$
$$J_{yn}(x, y) = |y - y_n|/l_y \qquad x_n - l_x < x < x_n + l_x,\quad y_n - l_y < y < y_n + l_y$$
$$= 0 \qquad \text{otherwise}$$

where x_n, y_n are the coordinates of the center of the nth element and l_x, l_y are the sizes of each finite element.

Their two dimensional discrete fourier transforms are

$$\tilde{J}_{xn}(n, m) = \frac{4}{\alpha^2 \beta l_x} \operatorname{Cos} \alpha x_n (1 - \operatorname{Cos} \alpha l_x) \cdot \operatorname{Sin} \beta y_n \operatorname{Sin} \beta l_y$$

$$\tilde{J}_{yn}(n, m) = \frac{4}{\alpha \beta^2 l_y} \operatorname{Cos} \beta y_n (1 - \operatorname{Cos} \beta l_y) \cdot \operatorname{Sin} \alpha x_n \operatorname{Sin} \alpha l_x$$

where $\alpha = n\pi/a$ and $\beta = m\pi/b$.

Now:

$$\tilde{Z}_{st}^{\infty} = \sum G_{ij}(n, m)\, J_{is}(n, m, x_s, y_s)\, J_{jt}(n, m, x_t, y_t)$$

where i and j represent the directions x or y depending on which component of the dyadic is required and the com-

ponents of the asymptotic Green's dyadic is given by [8]:

$$\frac{k_0}{Z_0}\tilde{G}^{\infty}_{xx} = \frac{\beta^2 k_0^2}{2(\alpha^2+\beta^2)^{3/2}} - \frac{\alpha^2}{(\alpha^2+\beta^2)^{1/2}(1+\epsilon)}$$

$$\frac{k_0}{Z_0}\tilde{G}^{\infty}_{xy} = -\frac{\alpha\beta}{(\alpha^2+\beta^2)^{1/2}(1+\epsilon)}$$

$$\frac{k_0}{Z_0}\tilde{G}^{\infty}_{yy} = \frac{\alpha^2 k_0^2}{2(\alpha^2+\beta^2)^{3/2}} - \frac{\beta^2}{(\alpha^2+\beta^2)^{1/2}(1+\epsilon)}$$

Taking the first quadrant of $\tilde{\boldsymbol{Z}}^{\infty}$, which corresponds to the xx component of the dyadic, as an example we get:

$$\tilde{Z}^{\infty}_{st} = 4\sum P(x_s, y_s, x_t, y_t)(Q_{xx1}(n, m) + Q_{xx2}(n, m))$$

where

$$P = \operatorname{Cos}\alpha x_s \operatorname{Sin}\beta y_s \operatorname{Cos}\alpha x_t \operatorname{Sin}\beta y_t$$

$$Q_{xx1} = \frac{4}{\alpha^4\beta^2 l_x^2}(1-\operatorname{Cos}\alpha l_x)^2 \operatorname{Sin}^2\beta l_y K^{\infty}_{xx1}(\alpha, \beta)$$

$$Q_{xx2} = \frac{4}{\alpha^4\beta^2 l_x^2}(1-\operatorname{Cos}\alpha l_x)^2 \operatorname{Sin}^2\beta l_y K^{\infty}_{xx2}(\alpha, \beta)$$

$$K^{\infty}_{xx1} = \frac{\beta^2}{(\alpha^2+\beta^2)^{3/2}} \quad \text{and} \quad K^{\infty}_{xx2} = \frac{\alpha^2}{(\alpha^2+\beta^2)^{1/2}}$$

Rearranging we have

$$P = 0.25(\operatorname{Cos}\alpha(x_s+x_t) + \operatorname{Cos}\alpha(x_s-x_t)) \cdot (-\operatorname{Cos}\beta(y_s+y_t) + \operatorname{Cos}\beta(y_s-y_t))$$

and Z^{∞}_{xx} is given by

$$J_{xx1}\Big(\sum - Q_{xx1}(n, m)\operatorname{Cos}\frac{n\pi u^+_{st}}{a}\operatorname{Cos}\frac{m\pi v^+_{st}}{b} + \sum Q_{xx1}(n, m)\operatorname{Cos}\frac{n\pi u^+_{st}}{a}\operatorname{Cos}\frac{m\pi v^-_{st}}{b} - \sum Q_{xx1}(n, m)\operatorname{Cos}\frac{n\pi u^-_{st}}{a}\operatorname{Cos}\frac{m\pi v^+_{st}}{b} + \sum Q_{xx1}(n, m)\operatorname{Cos}\frac{n\pi u^-_{st}}{a}\operatorname{Cos}\frac{m\pi v^-_{st}}{b}\Big)$$

$$J_{xx2}\Big(\sum - Q_{xx2}(n, m)\operatorname{Cos}\frac{n\pi u^+_{st}}{a}\operatorname{Cos}\frac{m\pi v^+_{st}}{b} + \sum Q_{xx2}(n, m)\operatorname{Cos}\frac{n\pi u^+_{st}}{a}\operatorname{Cos}\frac{m\pi v^-_{st}}{b} - \sum Q_{xx2}(n, m)\operatorname{Cos}\frac{n\pi u^-_{st}}{a}\operatorname{Cos}\frac{m\pi v^+_{st}}{b} + \sum Q_{xx2}(n, m)\operatorname{Cos}\frac{n\pi u^-_{st}}{a}\operatorname{Cos}\frac{m\pi v^-_{st}}{b}\Big)$$

where $u^+_{st} = x_s + x_t$, $v^+_{st} = y_s + y_t$.

$$J_{xx1} = k_0^2/2 \quad J_{xx2} = -1/(1+\epsilon)$$

and

$$G^{\infty}_{xx} = J_{xx1}K_{xx1} + J_{xx2}K_{xx2}$$

This is the sum of four terms each of the two dimensional discrete fourier transforms of $Q_1(n, m)$ and $Q_2(n, m)$ provided that

$$\frac{u^{\pm}_{st}(N+1)}{a} \quad \text{and} \quad \frac{v^{\pm}_{st}(N+1)}{b}$$

are integers for all s and t.

In a similar manner we find the other quadrants of $\boldsymbol{Z}$ as follows:

Z^{∞}_{xy} is given by

$$J_{xy}\Big(\sum - Q_{xy}(n, m)\operatorname{Cos}\frac{n\pi u^+_{st}}{a}\operatorname{Cos}\frac{m\pi v^+_{st}}{b} + \sum Q_{xy}(n, m)\operatorname{Cos}\frac{n\pi u^+_{st}}{a}\operatorname{Cos}\frac{m\pi v^-_{st}}{b} - \sum Q_{xy}(n, m)\operatorname{Cos}\frac{n\pi u^-_{st}}{a}\operatorname{Cos}\frac{m\pi v^+_{st}}{b} + \sum Q_{xy}(n, m)\operatorname{Cos}\frac{n\pi u^-_{st}}{a}\operatorname{Cos}\frac{m\pi v^-_{st}}{b}\Big)$$

Z^{∞}_{yy} is given by

$$J_{yy1}\Big(\sum - Q_{yy1}(n, m)\operatorname{Cos}\frac{n\pi u^+_{st}}{a}\operatorname{Cos}\frac{m\pi v^+_{st}}{b} + \sum Q_{yy1}(n, m)\operatorname{Cos}\frac{n\pi u^+_{st}}{a}\operatorname{Cos}\frac{m\pi v^-_{st}}{b} - \sum Q_{yy1}(n, m)\operatorname{Cos}\frac{n\pi u^-_{st}}{a}\operatorname{Cos}\frac{m\pi v^+_{st}}{b} + \sum Q_{yy1}(n, m)\operatorname{Cos}\frac{n\pi u^-_{st}}{a}\operatorname{Cos}\frac{m\pi v^-_{st}}{b}\Big)$$

$$\cdot J_{yy2}\Big(\sum - Q_{yy2}(n, m)\operatorname{Cos}\frac{n\pi u^+_{st}}{a}\operatorname{Cos}\frac{m\pi v^+_{st}}{b} + \sum Q_{yy2}(n, m)\operatorname{Cos}\frac{n\pi u^+_{st}}{a}\operatorname{Cos}\frac{m\pi v^-_{st}}{b} - \sum Q_{yy2}(n, m)\operatorname{Cos}\frac{n\pi u^-_{st}}{a}\operatorname{Cos}\frac{m\pi v^+_{st}}{b} + \sum Q_{yy2}(n, m)\operatorname{Cos}\frac{n\pi u^-_{st}}{a}\operatorname{Cos}\frac{m\pi v^-_{st}}{b}\Big)$$

where

$$J_{xy} = k_0^2/2$$

$$Q_{xy} = \frac{4}{\alpha^3\beta^3 l_x l_y}(1-\operatorname{Cos}\alpha l_x)\operatorname{Sin}\beta l_y(1-\operatorname{Cos}\beta l_y) \cdot \operatorname{Sin}\alpha l_x K^{\infty}_{xy}(\alpha, \beta)$$

$$K^{\infty}_{xy} = -\frac{\alpha\beta}{(\alpha^2+\beta^2)^{1/2}}$$

$$J_{yy1} = -k_0^2/2 \quad J_{yy2} = 1/(1+\epsilon)$$

$$Q_{yy1} = \frac{4}{\alpha^2\beta^4 l_y^2}(1 - \mathrm{Cos}\,\beta l_y)^2\,\mathrm{Sin}^2\,\alpha l_x K^{\infty}_{yy1}(\alpha, \beta)$$

$$Q_{yy2} = \frac{4}{\alpha^2\beta^4 l_y^2}(1 - \mathrm{Cos}\,\beta l_y)^2\,\mathrm{Sin}^2\,\alpha l_x K^{\infty}_{yy2}(\alpha, \beta)$$

$$K^{\infty}_{yy1} = \frac{\alpha^2}{(\alpha^2+\beta^2)^{3/2}} \quad \text{and} \quad K^{\infty}_{yy2} = \frac{\beta^2}{(\alpha^2+\beta^2)^{1/2}}.$$

Thus, by calculating the two dimensional FFT of the five functions Q, which are independent of the metallisation of the circuit under investigation, we may speedily calculate all the elements of $\mathbf{Z}^{\infty}$.

References

[1] R. W. Jackson, "Full-wave finite element analysis of irregular microstrip discontinuities," *IEEE Trans. Microwave Theory Tech.*, vol. 37, pp. 81–89, Jan. 1989.

[2] A. Hill and V. K. Tripathi, "An efficient algorithm for the three dimensional analysis of passive microstrip components and discontinuities for microwave and millimeter wave integrated circuits," *IEEE Trans. Microwave Theory Tech.*, vol. 39, pp. 83–91, Jan. 1991.

[3] K. S. Yee, "Numerical solution of initial boundary value problems involving Maxwell's equations in isotropic media," *IEEE Trans. Antennas Propagat.*, vol. 14, no. 3, pp. 302–307, 1966.

[4] J. Uher, S. Liang, and W. J. R. Hoeffer, "S-parameters of microwave components computed with the 3-D condensed symmetrical TLM Node," in *1990 IEEE MTT-S Int. Microwave Symp. Dig.*, Dallas, TX, pp. 653–656.

[5] S. Koike, N. Yoshida, and I. Fukai, "Transient analysis of coupling between crossing lines in three-dimensional space," *IEEE Trans. Microwave Theory Tech.*, vol. 35, pp. 67–71, Jan. 1987.

[6] W. P. Harokopus and L. P. B. Katehi, "Electromagnetic coupling and radiation loss considerations in microstrip (M)MIC design," *IEEE Trans. Microwave Theory Tech.*, vol. 39, pp. 413–421, Mar. 1991.

[7] W. Wertgen and R. H. Jansen, "Novel Green's function database technique for the efficient full-wave analysis of complex irregular (M)MIC structures," in *Proc. 19th European Microwave Conf.*, London, 1989, pp. 199–204.

[8] C. J. Railton and J. P. McGeehan, "A rigorous and computationally efficient analysis of microstrip for use as an electro-optic modulator," *IEEE Trans. Microwave Theory Tech.*, vol. 37, pp. 1099–1104, July 1989.

[9] C. J. Railton and J. P. McGeehan, "Analysis of MMIC components including the effect of finite metallisation thickness," in *Proc. 19th European Microwave Conf.*, London, 1989, pp. 187–192.

[10] C. J. Railton and T. Rozzi, "Complex modes in boxed microstrip," *IEEE Trans. Microwave Theory Tech.*, vol. 36, pp. 865–874, May 1988.

[11] T. Shibata, T. Hayashi, and T. Kimura, "Analysis of microstrip circuits using three-dimensional full-wave electromagnetic field analysis in the time domain," *IEEE Trans. Microwave Theory Tech.*, vol. 36, pp. 1064–1070, June 1988.

[12] D. Paul, E. M. Daniel, and C. J. Railton, "Fast finite difference time domain method for the analysis of a planar microstrip filter," in *Proc. European Microwave Conf.*, 1991, Stuttgart, pp. 303–308.

C. J. Railton (M'88) received the B.Sc. degree (with honours) in physics with electronics from the University of London, England in 1974 and the Ph.D. degree in electronic engineering from the University of Bath, England in 1988.

During the period 1974–1984 he worked in the scientific civil service on a number of research and development projects in the areas of communications and signal processing. Between 1984 and 1987 he worked at the University of Bath on the mathematical modeling of boxed microstrip circuits. Dr. Railton currently works in the Communications Research Centre at the University of Bristol where he leads a group involved in the mathematical modeling and development of CAD tools for MMIC's, planar antennas, microwave heating systems, EMC and high speed logic.

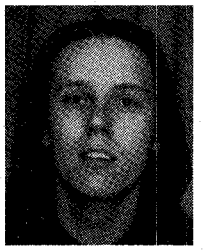

S. A. Meade was born in Taunton, Somerset, England in 1968. He received the B.Eng. degree (with honours) in electrical and electronic engineering from the University of Bristol in 1990. He is currently pursuing the Ph.D. degree at the Communications Research Centre, University of Bristol.

His research interests include the application of spectral domain method to modeling of complex planar circuits.